Plant Physiol. (1994) 105: 435–442

Methylammonium as a Transport Analog for Ammonium in Tomato (*Lycopersicon esculentum* L.)[1]

Kevin R. Kosola[2]* and Arnold J. Bloom

Vegetable Crops Department, University of California, Davis, Davis, California 95616–8746

Methylammonium ($CH_3NH_3^+$) has been widely used as an analog of ammonium (NH_4^+) for examining transport in bacteria and fungi. We compared the kinetics of root $CH_3NH_3^+$ and NH_4^+ uptake from solution culture in intact tomato (*Lycopersicon esculentum* cv T5) plants. Efflux of NH_4^+ and $CH_3NH_3^+$ was negligible. The apparent maximum rate of absorption (apparent V_{max}) was similar for NH_4^+ and $CH_3NH_3^+$, but the apparent affinity (apparent K_m) was about 10-fold greater for NH_4^+ than for $CH_3NH_3^+$. In characterizing the interaction between NH_4^+ and $CH_3NH_3^+$ transport, we used [^{15}N]-NH_4^+ and [^{14}C]$CH_3NH_3^+$ as well as improved methods for analysis of nonisotopic $CH_3NH_3^+$ and NH_4^+. $CH_3NH_3^+$ acted as an inhibitor of NH_4^+ influx. Relatively low concentrations of NH_4^+ strongly inhibited $CH_3NH_3^+$ influx. Treatments with 1 mM methionine sulfoximine that blocked NH_4^+ assimilation had little influence on NH_4^+ inhibition of $CH_3NH_3^+$ influx. These results suggest that the two ions share a common transport system in tomato, but because this transport system has a much greater affinity for NH_4^+, $CH_3NH_3^+$ may be used as a transport analog only when ambient concentrations of NH_4^+ are very low.

Ammonium (NH_4^+) is a major source of mineral nitrogen in many soils, yet ammonium uptake by plants has received relatively little attention (Kleiner, 1981), in part due to the lack of appropriate methods. In solution culture, NH_4^+ uptake has been analyzed by measuring the depletion of NH_4^+ (Bloom and Chapin, 1981) or by using the tracers [^{15}N]NH_4^+ (Macklon et al., 1990), [^{13}N]NH_4^+ (McNaughton and Presland, 1983; Wang et al., 1993), or [^{14}C]$CH_3NH_3^+$ (Jackson and Caldwell, 1992). There are problems with each of these tracers: [^{15}N]NH_4^+ may be converted to [^{15}N]NO_3^- by soil microorganisms, [^{13}N]NH_4^+ has a half-life of 10 min, and [^{14}C]$CH_3NH_3^+$ has not been shown to be a transport analog for NH_4^+ in higher plants. There are some potential advantages to using [^{14}C]$CH_3NH_3^+$ as a tracer; unlike [^{15}N]NH_4^+, [^{14}C]$CH_3NH_3^+$ is not converted to labeled NO_3^- or a labeled analog of NO_3^- by microorganisms (Holtel and Kleiner, 1985). [^{14}C]$CH_3NH_3^+$ is commercially available and can be detected by liquid scintillation counting at extremely low levels.

Many organisms appear to have a common uptake system for $CH_3NH_3^+$ and NH_4^+. In several fungi, conditions that induce NH_4^+ uptake also induce $CH_3NH_3^+$ uptake (Hackette et al., 1970; Arst and Page, 1973; Pateman et al., 1973; Roon et al., 1975). Fungal mutants deficient in $CH_3NH_3^+$ transport are also deficient in NH_4^+ transport (Arst and Page, 1973; Pateman et al., 1974; Roon et al., 1975). In the unicellular alga *Chlorella*, a single-gene mutant has been described that is deficient in both $CH_3NH_3^+$ and NH_4^+ uptake but not ethylammonium uptake (Franco et al., 1987).

Competition between $CH_3NH_3^+$ and NH_4^+ during influx also indicates that the two ions share a common transport system, but detailed kinetics studies are limited. The influence of $CH_3NH_3^+$ on NH_4^+ influx has been examined only in a study of *Chara corallina*, in which 100 μM $CH_3NH_3^+$ did not significantly inhibit NH_4^+ influx at 20 or 100 μM (Walker et al., 1979b). By contrast, NH_4^+ inhibits $CH_3NH_3^+$ uptake in many bacteria and cyanobacteria (Boussiba et al., 1984; Holtel and Kleiner, 1985) and in fungi (Hackette et al., 1970; Cook and Anthony, 1978).

The following study characterized the kinetics of root $CH_3NH_3^+$ uptake and interactions between root $CH_3NH_3^+$ and NH_4^+ influx in a higher plant, *Lycopersicon esculentum* Mill. cv T5. We developed methods using a CH_3NH_2 electrode and MPIC for analysis of $CH_3NH_3^+$. With these techniques, $CH_3NH_3^+$ could be used as a tracer without requiring the use of radioactively labeled material.

MATERIALS AND METHODS

Growth and Acclimation Conditions

Tomato (*Lycopersicon esculentum* Mill. cv T5) seeds were placed in germination paper saturated with 1 mM $CaSO_4$ and kept at approximately 24°C. Five days after germination, 6 or 20 seedlings were transferred to an opaque root box containing 1.5 or 4.8 L, respectively, of a well-aerated modified Hoagland solution, pH 7.0 (Epstein, 1972). The composition of the nutrient solution was 150 μM $NH_4H_2PO_4$, 150 μM KNO_3, 2 mM $CaSO_4$, 1 mM $MgSO_4$, 650 μM K_2HPO_4, 350 μM KH_2PO_4, 600 μM K_2SO_4, 20 μM Fe-EDTA, 50 μM KCl, 25 μM H_3BO_3, 2 μM $MnSO_4$, 2 μM $ZnSO_4$, 0.5 μM $CuSO_4$, and 0.5 μM H_2MoO_4. Plants were grown for 6 d under low-light intensities and then transferred to a greenhouse. The root boxes were suspended in a water bath that kept root temperature at 20 ± 0.1°C; the shoot temperature was approximately 27°C day/19°C night, and daytime light intensity was

[1] Supported in part by National Science Foundation grants BSR-8821255 and DCB-8916637 to A.J.B.

[2] Present address: Michigan State University, Kellogg Biological Station, 3700 E. Gull Lake Drive, Hickory Corners, MI 49060.

* Corresponding author; fax 1–616–671–2104.

Abbreviations: DTPA, diaminetriaminepentaacetic acid; MPIC, mobile phase ion chromatography; MSX, L-methionine sulfoximine.

400 to 1500 μmol photons m^{-2} s^{-1} PAR. The nutrient solution was supplemented daily with $NH_4H_2PO_4$ and KNO_3 to maintain solution concentrations at 150 ± 50 μeq NH_4^+ and NO_3^-.

Three-week-old plants with two fully expanded leaves were transferred from the greenhouse to a measurement system in the laboratory the night before an experiment. The measurement system has been described previously (Bloom, 1989). A slotted rubber stopper was fitted around the stem of each plant; the roots were carefully placed in the stainless steel mesh basket inside a root cuvette, and the stopper was sealed in the top of the cuvette. The multichamber system contained 12 temperature-controlled root cuvettes (Fig. 1). This system allowed removal of any number and combination of chambers from the solution path without altering flow in the other root cuvettes. Flow from a single-piston pump (Fluid Metering, Inc., Oyster Bay, NJ) to the cuvettes was controlled by an array of two-way solenoid valves (Angar Scientific, Cedar Knolls, NJ) that were connected to a digital manifold controller. The digital manifold controller (schematic available) acted to send each piston stroke of the pump to a different chamber; if the cuvette was off-line, the overflow solenoid was activated, and the solution from that piston stroke was returned to the main solution reservoir. This system allowed simultaneous maintenance of up to 12 plants under well-defined conditions for labeling or uptake studies.

Plants were exposed overnight to a flowing solution containing 5 μM NH_4Cl, 1.6 mM $CaSO_4$, and 0.5 μM K_2HPO_4. In the morning, the flowing solution was changed according to the experimental protocols described below. The roots were kept at 20°C and in the dark; the shoots were exposed to an ambient temperature of 24°C and, during the day, to a PPFD of 600 μmol photons m^{-2} s^{-1}.

Concentration Dependence of Net NH_4^+ and $CH_3NH_3^+$ Flux

In experiments on the kinetics of net $CH_3NH_3^+$ or NH_4^+ flux, plants received a nutrient solution containing 1 mM Na_2SO_4 to adjust ionic strength, 0.5 mM $CaSO_4$, 0.5 μM K_2HPO_4, and varying concentrations of either CH_3NH_3Cl or NH_4Cl. The pH of this unbuffered solution was adjusted to about pH 6.8 by addition of 1 M NaOH. The nutrient solution was discarded after a single pass through the root cuvette. NH_4^+ depletion was measured with an ammonia gas-sensing electrode (Orion model 9512) containing a filling solution of 100 mM NH_4Cl saturated with Ag^+. To measure $CH_3NH_3^+$ depletion, the electrode-filling solution was changed to 10 mM CH_3NH_3Cl saturated with Ag^+. A syringe pump added sufficient 10 M NaOH to the sample solution stream to bring the pH to 13 and convert NH_4^+ or $CH_3NH_3^+$ to their unprotonated gaseous forms (Bloom, 1989). Because NH_4^+ and $CH_3NH_3^+$ mutually interfere with the response of each type of electrode, this method was used to analyze solutions containing only one ion or the other.

Each plant was exposed to a series of increasing concentrations of NH_4Cl or CH_3NH_3Cl (5, 10, 20, 50, 100, 200, and 500 μM) and held at each concentration until depletion from the nutrient solution reached a steady rate (Bloom, 1989). As a control for possible circadian variation in $CH_3NH_3^+$ uptake and for long-term effects of $CH_3NH_3^+$ exposure, depletion from 50 μM $CH_3NH_3^+$ was monitored continuously for 12 h under these experimental conditions.

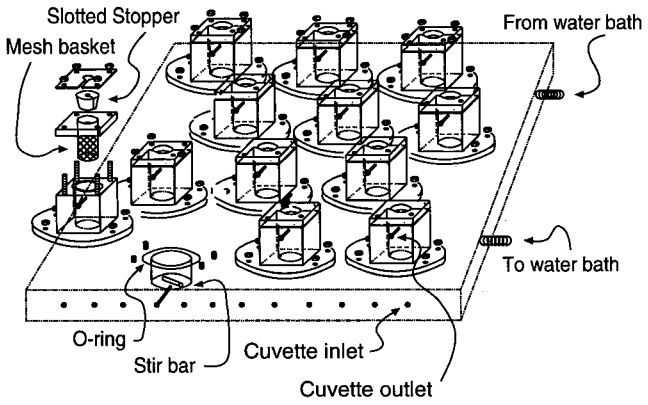

Figure 1. Schematic of the multichamber solution culture system.

Interactions between NH_4^+ and $CH_3NH_3^+$

Suppressed and unsuppressed MPIC (Small, 1989) was used to measure $CH_3NH_3^+$ and NH_4^+ concentrations in solutions containing both ions. To avoid Na^+ interference with the NH_4^+ peak in suppressed MPIC, $CaSO_4$ was substituted for Na_2SO_4 in the nutrient solution supplied to the plant, giving a background solution of 1.6 mM $CaSO_4$ and 0.5 μM K_2HPO_4. To assess the influence of $CH_3NH_3^+$ on NH_4^+ uptake, the plant was exposed to a series of increasing concentrations of NH_4Cl (10, 20, 50, 100, 200, and 500 μM) under a constant background of 50 μM CH_3NH_3Cl; to assess the influence of NH_4^+ inhibition on $CH_3NH_3^+$ uptake, the plant was exposed to a series of increasing concentrations of CH_3NH_3Cl (10, 20, 50, 100, 200, and 500 μM) under a constant background of 10 μM NH_4^+. Because the roots absorbed NH_4^+ at high rates, 17 μM NH_4^+ was supplied in the inlet solution stream to maintain a concentration of 10 μM NH_4^+ in the root cuvette. For both studies, a sample was collected at each concentration when net uptake of NH_4^+ and $CH_3NH_3^+$ reached a steady rate, as indicated by monitoring with the NH_3 and CH_3NH_2 electrodes. All samples were sealed and stored at 5°C for subsequent MPIC analysis. NH_4^+ and $CH_3NH_3^+$ concentrations in solutions of known composition did not change over time with such treatment.

MPIC Analysis of Samples

A Dionex NS-1 MPIC column in a metal-free Dionex ion chromatography system was used to separate $CH_3NH_3^+$ and NH_4^+. Three variations of MPIC analysis were compared. Two methods used a Dionex CMMS-1 suppressor column with different pairs of eluents and regenerants. A suppressor column, when supplied with the appropriate regenerant solution, reduces the background eluent conductivity, enabling detection of low levels of the analyte (Small, 1989). The eluents and regenerants used here were either a 1 mM octanesulfonic acid eluent (flow rate 1.0 mL min^{-1}) with a 25 mM tetrabutylammonium hydroxide regenerant (flow rate 2.5 mL

min^{-1}) or a 5 mM hexanesulfonic acid plus 40 mM H_3BO_3 eluent (flow rate 1.0 mL min^{-1}) with a 25 mM tetrabutylammonium hydroxide plus 30 mM H_3BO_3 regenerant (flow rate 6 mL min^{-1}).

The third, most satisfactory approach did not require a suppressor column because it used a detector specific to NH_3 and CH_3NH_2 and other volatile amines (Carlson, 1978). Samples were passed through the MPIC column with an eluent of 4 mM octanesulfonic acid (flow rate 1.1 mL min^{-1}) for separation (Fig. 2). Downstream of the column, the eluent was mixed with 2.5 N NaOH and 50 mM DTPA (flow rate 0.3 mL min^{-1}); the NaOH converted $CH_3NH_3^+$ and NH_4^+ to the gaseous unprotonated forms CH_3NH_2 and NH_3, and the DTPA prevented precipitation of CaOH. The alkaline eluent stream was then passed through one channel of a diffusion exchange module (Wescan model 360). CH_3NH_2 and NH_3 diffused from the alkaline eluent stream through the Teflon membrane of the module and dissolved into the water flowing through the other channel of the module (flow rate 1.14 mL min^{-1}). The measured conductivity of this water increased linearly with increasing sample concentration of $CH_3NH_3^+$ and NH_4^+.

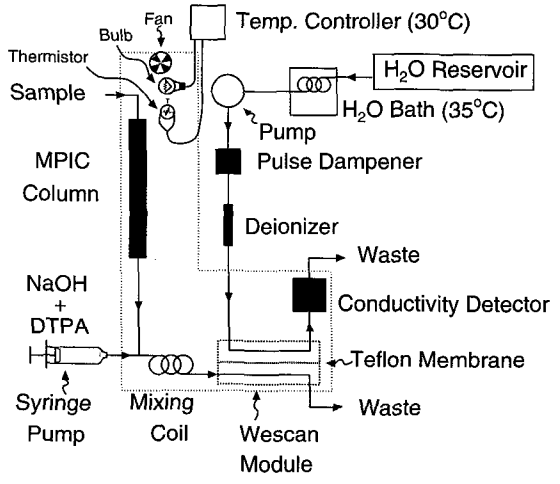

Figure 2. Diagram of the MPIC system attached to the amine diffusion exchange detector for analysis of NH_4^+ and $CH_3NH_3^+$. The Wescan diffusion exchange module is from the Wescan model 360 ammonia analyzer (Alltech Associates, Inc., Deerfield, IL). The MPIC system consisted of a Dionex MPIC column and conductivity detector (Dionex Corp., Sunnyvale, CA) with a 200-μL sample injection loop. Use of a 200-μL sample loop gave good sensitivity at low sample concentrations but necessitated the use of an eluent giving greater peak separation and longer retention times. The MPIC eluent was 4 mM octanesulfonic acid pumped at a flow rate of 1.1 mL min^{-1}. The alkaline solution was 2.5 N NaOH plus 50 mM DTPA (as a chelator), delivered at a flow rate of 0.3 mL min^{-1} from a Razel A99-HM syringe pump (Razel Scientific Instruments, Inc., Stamford, CT) fitted with a 60-mL plastic syringe. Distilled deionized water was heated to 35°C and pumped to the diffusion exchange module at 1.14 mL min^{-1} by a FMI RH pump in line with a FMI PD-60-LF pulse dampener (Fluid Metering, Inc.). The pulse dampener was insulated to reduce temperature variation in the water supplied to the diffusion exchange module. The water passed through a 1-mL syringe filled with Bio-Rad AG501-X8(D) resin to ensure a low background conductivity. The diffusion exchange module, MPIC column, mixing coil, and conductivity detector were all enclosed in a temperature-controlled Plexiglas cabinet (dotted line) at 30°C. The configuration shown, with the water and alkaline eluent flowing through the diffusion exchange module in the same direction, gave greater recovery of CH_3NH_2 and NH_3 than a countercurrent flow of water and basic eluent.

[^{14}C]$CH_3NH_3^+$ Influx

Twelve plants were placed overnight in the multiplant system with 5 μM NH_4Cl, 1.6 mM $CaSO_4$, and 0.5 μM K_2HPO_4 flowing through the root cuvettes at a rate of approximately 1.5 mL min^{-1}. Each cuvette had a total volume of about 70 mL. Shoot and root conditions were as described for measurements of net flux. Before the labeling protocol was begun, the solution was switched to 1.6 mM $CaSO_4$ and 0.5 μM K_2HPO_4 to flush NH_4^+ from the root chambers; plants were then maintained on this NH_4^+-free solution for between 1 and 4 h.

At the start of the labeling period for each plant, solution flow to the cuvette was stopped and an aliquot of [^{14}C]-CH_3NH_3Cl was injected into the chamber, bringing the solution to a concentration of 500 μM [^{14}C]CH_3NH_3Cl. After 2.5, 5, 7.5, 10, 12.5, or 15 min, the plants were removed and the roots were immersed briefly (5–10 s) in 300 mL of deionized water at room temperature to rinse off surface radioactivity and then placed in 70 mL of ice-cold 1.6 mM $CaSO_4$ and 0.5 μM K_2HPO_4 for 1 min to rinse label out of the apoplast. Because calcium was included in the labeling and rinse solution, it was not considered necessary to add NH_4^+ or $CH_3NH_3^+$ to the rinse solution; as a divalent cation, calcium should have a higher affinity for nonspecific cation-binding sites in the cell wall than either NH_4^+ or $CH_3NH_3^+$. After the roots were blotted briefly, roots and shoots were separated and placed in glass scintillation vials. The samples were oven dried for at least 24 h at 50°C, weighed, and then cut into 2-mm pieces. Each sample received 3 mL of boiling water and was soaked for at least 30 min before receiving 15 mL of scintillation fluid (Bio-Safe II, Research Products International Corp., Mt. Prospect, IL). Samples were analyzed with a Beckman LS7000 liquid scintillation counter and correction was made for quenching.

The linear increase in [^{14}C]$CH_3NH_3^+$ accumulation with time from 2.5 to 15 min (regression: $y = 2.635(x) + 0.195$; $r^2 = 0.99$; $n = 1$ for each point) indicates that efflux was not significant during this period. We therefore chose a labeling period of 10 min for subsequent experiments. The rinsing protocol appeared to be appropriate, because the intercept with the y axis was not significantly different from zero ($P = 0.45$). Any retention of apoplastic label during rinsing would cause the intercept with the y axis to be greater than zero; rinse periods that were too long would shift the y intercept to negative values.

To determine the concentration dependence of [^{14}C]-$CH_3NH_3^+$ influx in the presence and absence of 10 μM NH_4^+, plants were acclimated overnight as described above and then exposed to 10, 20, 50, 100, 200, or 500 μM [^{14}C]$CH_3NH_3^+$ in the presence or absence of 10 μM NH_4^+ for 10-min labeling periods. Root and shoot tissues were sampled and prepared for scintillation counting as described above.

The effects of exposure to MSX (Sigma M5379) on [^{14}C]-$CH_3NH_3^+$ influx in the presence or absence of 10 μM NH_4^+ were also examined. After the standard overnight acclimation, plants were exposed to a flowing solution containing 1 mM MSX, 1.6 mM $CaSO_4$, and 0.5 μM K_2HPO_4 flowing through the cuvettes at a rate of approximately 1.0 mL min^{-1} for at least 2 h before [^{14}C]$CH_3NH_3^+$ labeling. As a check on the efficacy of 1 mM MSX in altering NH_4^+ metabolism, changes in soluble amino acids were measured in plants exposed to 1 mM MSX, 5 μM NH_4^+, 1.6 mM $CaSO_4$, and 0.5 μM K_2HPO_4 flowing at an approximate rate of 1.3 mL min^{-1} for 0, 2, 4, or 6 h. Soluble amino acids were extracted separately from root and shoot samples by the method of Bieleski and Turner (1966). Amino acid analysis was performed by the University of California, Davis, Protein Structure Laboratory with a Beckman 6300 amino acid analyzer.

[^{15}N]NH_4^+ Influx

Experimental protocols for measurements of [^{15}N]NH_4^+ influx were the same as those used for measurements of [^{14}C]$CH_3NH_3^+$ influx, with the exception that plants were exposed to 10, 20, 50, 100, 200, or 500 μM [^{15}N]NH_4^+. After the plants were dried at 50°C and weighed, the root and shoot from each were combined and ground to a flour-like consistency in a Wiggl-Bug miniature ball mill (Crescent Dental Manufacturing, Lyons, IL) and then analyzed for ^{15}N and percentage of nitrogen content by combined elemental analysis and MS (Isotope Services, Los Alamos, NM).

[^{15}N]NH_4^+ influx was also measured in the presence of 100 or 500 μM $CH_3NH_3^+$. Root and shoot tissues were sampled and prepared for analysis as described above.

Data Analysis

Analysis of variance was performed on influx or net flux rates at each substrate concentration using the SAS GLM procedure (Freund et al., 1986); a priori means separation was carried out using Duncan's multiple range test (Freund et al., 1986). This analysis tests the null hypothesis that two sets of net flux or influx data are not significantly different from one another. Interpretation of the analysis of variance does not depend on any assumptions about the mechanisms behind the differences.

Goodness of fit of the kinetics data to the Michaelis-Menten model was tested by linear regression analysis of data transformed by the Woolf-Augustinsson-Hofstee method (abscissa = $V/[S]$, ordinate = V; Segel, 1976). This tests the null hypothesis that the simple Michaelis-Menten model is sufficient to account for the observed uptake kinetics. The Woolf-Augustinsson-Hofstee method avoids the weighting problems of the Lineweaver-Burk transformation (Segel, 1976).

Apparent K_m and V_{max} values were derived from the mean values for NH_4^+ and $CH_3NH_3^+$ influx or net flux by the hyperbolic regression analysis method of Wilkinson (1961). The SE values derived from this analysis include error due to both experimental variation and departure of the data from Michaelis-Menten kinetics.

RESULTS

MPIC Analytical Methods

All three MPIC methods for analysis of NH_4^+ and $CH_3NH_3^+$ concentrations provided similar readings with equal sensitivity and repeatability; typical background noise was equivalent to measurement variations of ±0.5 μM. The methods differed primarily in analysis time and cost of materials. The suppressed MPIC methods differed in that the retention times for NH_4^+ and $CH_3NH_3^+$ were much shorter for the hexanesulfonic acid eluent (Fig. 3A; NH_4^+ retention time = 9 min; $CH_3NH_3^+$ retention time = 10.5 min) than for the octanesulfonic acid eluent (NH_4^+ retention time = 40 min; $CH_3NH_3^+$ retention time = 47 min); each gave equally good separation between K^+, NH_4^+, and $CH_3NH_3^+$. Substitution of Ca^{2+} for Na^+ in the nutrient solution had no significant effect on NH_4^+ or $CH_3NH_3^+$ net flux but was necessary to avoid interference from the large Na^+ peak with the NH_4^+ and $CH_3NH_3^+$ peaks in each of these suppressed MPIC methods.

The main disadvantage with the suppressed MPIC methods was that Ca^{2+} interference greatly slowed sample analysis. The Ca^{2+} peak retention time was about 1 h with the hexanesulfonic acid eluent; after six samples were analyzed sequentially in 1 h, it was necessary to wait an additional 1

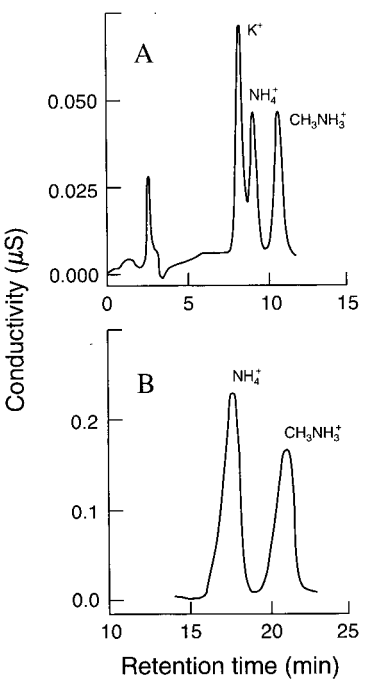

Figure 3. Chromatograms showing the separation between 0.5 μM K^+, 13 μM NH_4^+, and 20 μM $CH_3NH_3^+$ using a Dionex MPIC system with different eluents and different postseparation detection systems. A, Suppressed MPIC; the eluent is 5 mM hexanesulfonic acid plus 40 mM H_3BO_3. A 50-μL sample loop was used for this sample. B, Detection of NH_4^+ and $CH_3NH_3^+$ with the diffusion exchange module eliminates interference from K^+; the eluent used with this system is 4 mM octanesulfonic acid. A 200-μL sample loop was used for this sample.

h for the six calcium peaks to clear the column before more samples could be analyzed. Because the specific conductivity observed for K^+ was much greater than that of the amines (Fig. 3A) and the retention time for K^+ (8.12 min) was similar to that for NH_4^+ (8.94 min), interference from K^+ could prove problematic when analyzing NH_4^+ and $CH_3NH_3^+$ in samples with high K^+ concentrations, such as plant tissue extracts.

The amine diffusion detector avoided these problems. Only $CH_3NH_3^+$ and NH_4^+ were detected (Fig. 3B). Moreover, the cost of materials was much less because no suppression column solutions were necessary, and analysis time was shorter because we did not need to wait for the Ca^{2+} peak to clear the column.

NH_4^+ and $CH_3NH_3^+$ Transport

Linear regressions of the Woolf-Augustinsson-Hofstee transformed data were significant in most cases (Figs. 4–6, Table I). NH_4^+ net flux and $[^{15}N]NH_4^+$ influx were not signif-

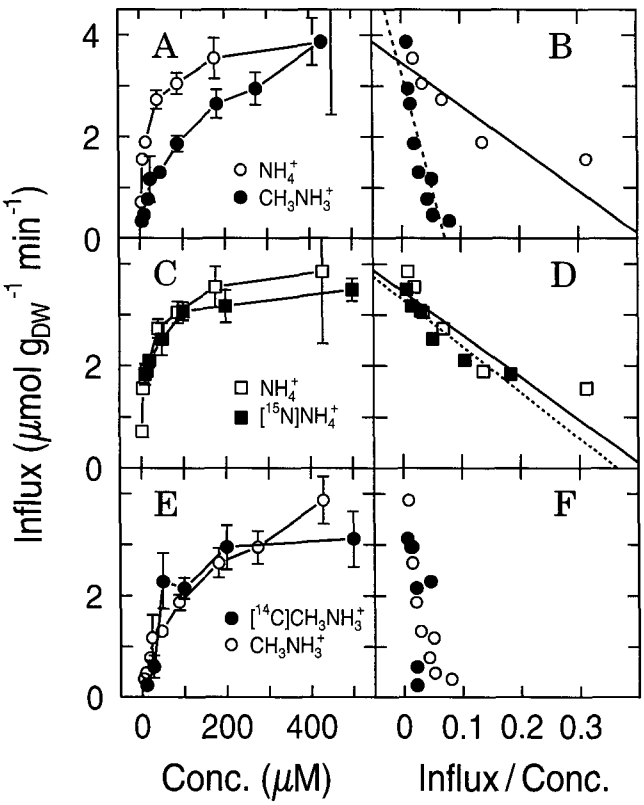

Figure 4. Dependence of NH_4^+ influx on NH_4^+ concentration and $CH_3NH_3^+$ influx on $CH_3NH_3^+$ concentration. Influx values are calculated per gram dry weight (DW) of root. Shown are means ± SE with small error bars incorporated into the symbols. A, $CH_3NH_3^+$ and NH_4^+ net flux; values are from steady-state depletion measurements; $n = 4$ for all NH_4^+ data; $n = 3$ for 300 and 500 μM $CH_3NH_3^+$; $n = 10$ to 16 for all other $CH_3NH_3^+$ data. B, Woolf-Augustinsson-Hofstee plot (abscissa = $V/[S]$, ordinate = V) of data presented in A. C, NH_4^+ net flux and $[^{15}N]NH_4^+$ influx; $n = 4$. D, Woolf-Augustinsson-Hofstee plot of data presented in C. E, $CH_3NH_3^+$ net flux and $[^{14}C]CH_3NH_3^+$ influx; $n = 4$. F, Woolf-Augustinsson-Hofstee plot of data presented in E.

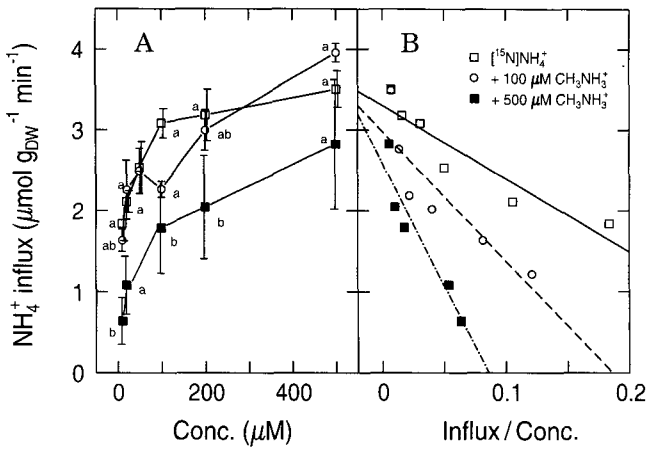

Figure 5. Inhibition of $[^{15}N]NH_4^+$ influx by 100 or 500 μM $CH_3NH_3^+$. Influx values are calculated per gram dry weight (DW) of root. Shown are the means ± SE with small error bars incorporated into the symbols. A, $[^{15}N]NH_4^+$ influx in the presence of 0, 100, or 500 μM $CH_3NH_3^+$; $n = 4$ for all data. Values for $[^{15}N]NH_4^+$ influx in the presence of $CH_3NH_3^+$ are significantly different from corresponding values for $[^{15}N]NH_4^+$ influx in the absence of $CH_3NH_3^+$ at the $P < 0.05$ level (Duncan's multiple range test) if they are marked with different letters. B, Woolf-Augustinsson-Hofstee plot (abscissa = $V/[S]$, ordinate = V) of the data presented in A.

icantly different across the concentration range examined (Table I; Fig. 4C; $P > 0.26$). Similarly, $CH_3NH_3^+$ net flux and $[^{14}C]CH_3NH_3^+$ influx were not significantly different (Fig. 4E; $P > 0.44$). The apparent K_m for NH_4^+ influx was about 10-fold less than that for $CH_3NH_3^+$ influx (Table I; Fig. 4, D and F).

The presence of 500 μM $CH_3NH_3^+$ significantly inhibited NH_4^+ influx at low concentrations (Fig. 5), acting to increase the apparent K_m (Table I). The presence of NH_4^+ significantly inhibited net flux and influx of $CH_3NH_3^+$ (Fig. 6). The addition of 10 μM NH_4^+ decreased the apparent V_{max} of both net flux and influx of $CH_3NH_3^+$ (Table I), significantly decreasing $CH_3NH_3^+$ net flux and influx at higher concentrations but not at the lowest concentrations (Fig. 6). The addition of 40 μM NH_4^+ inhibited $CH_3NH_3^+$ net flux significantly at all concentrations (Fig. 6A), decreasing the apparent V_{max} for net $CH_3NH_3^+$ flux even more than the addition of 10 μM NH_4^+. Treatment with 1 mM MSX apparently altered shoot and root NH_4^+ metabolism; shoot and root NH_4^+ concentrations increased, and root Gln and shoot Glu decreased (Fig. 7). There was no significant effect of MSX treatment on NH_4^+ inhibition of $[^{14}C]CH_3NH_3^+$ influx (Fig. 8).

DISCUSSION

Our results indicate that NH_4^+ and $CH_3NH_3^+$ share a common transport system in tomato roots. The primary evidence is that exposure to NH_4^+ and $CH_3NH_3^+$ reciprocally inhibited influx of the other ion. With a common transport system, this inhibition should be competitive. $CH_3NH_3^+$ inhibition of NH_4^+ absorption appears to be primarily competitive in that the V_{max} values for NH_4^+ influx under 0, 100,

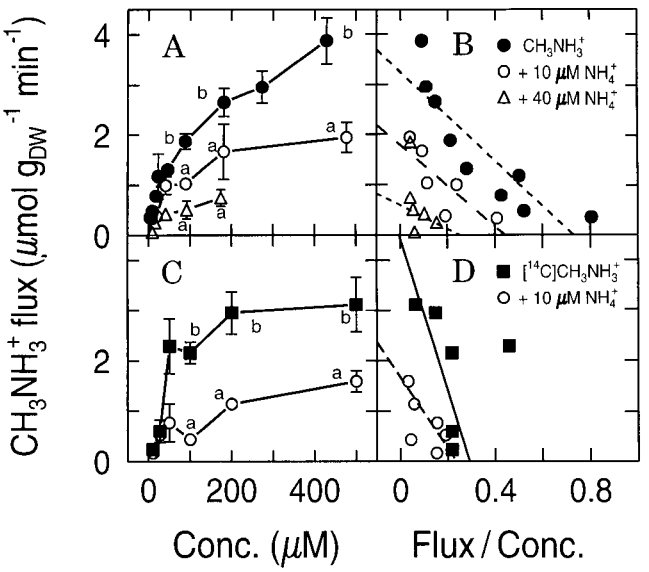

Figure 6. Inhibition of $CH_3NH_3^+$ influx by 10 or 40 μM NH_4^+. Influx values are calculated per gram dry weight (DW) of root. Shown are the means ± SE with small error bars incorporated into the symbols. A, $CH_3NH_3^+$ net flux in the presence of 0, 10, or 40 μM NH_4^+; n = 3 for 300 and 500 μM $CH_3NH_3^+$ net flux data; n = 4 for all data for $CH_3NH_3^+$ with 40 μM NH_4^+; n = 10 to 16 for all other net flux data. Values for $CH_3NH_3^+$ influx in the presence of NH_4^+ are significantly different from corresponding values for $[^{15}N]NH_4^+$ influx in the absence of $CH_3NH_3^+$ at the $P < 0.05$ level (Duncan's multiple range test) if they are marked with different letters. B, Woolf-Augustinsson-Hofstee plot (abscissa = $V/[S]$, ordinate = V) of the data presented in A. C, $[^{14}C]CH_3NH_3^+$ influx with and without 10 μM NH_4^+; n = 3 for all data. D, Woolf-Augustinsson-Hofstee plot of the data presented in C.

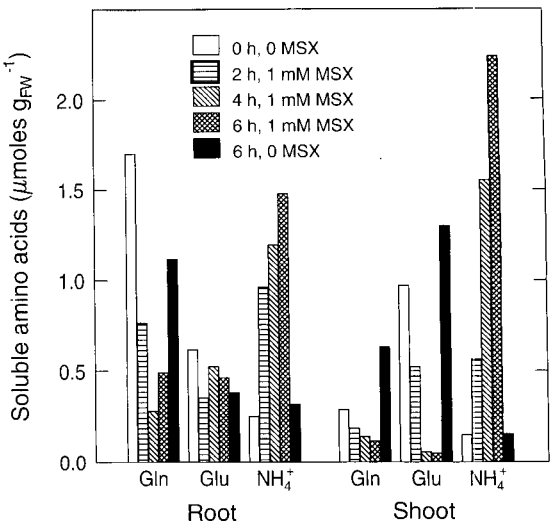

Figure 7. Shoot and root Gln, Glu, and NH_4^+ contents (nmol g^{-1} fresh weight [FW]) with varying exposure to MSX. Shown for each amino acid are values from time 0 (no exposure to MSX), values from plants exposed to MSX for 2, 4, and 6 h, and values from plants under the same experimental conditions for 6 h with no exposure to MSX. n = 1 for all data; three plants were pooled for each sample.

and 500 μM $CH_3NH_3^+$ are not significantly different ($P > 0.1$; Fig. 5B; Table I). By contrast, $CH_3NH_3^+$ absorption does not adequately fit simple Michaelis-Menten kinetics to determine unequivocally the type of inhibition by NH_4^+ (Fig. 6). This in part derives from difficulties in measuring $CH_3NH_3^+$ absorption while maintaining a constant background of 10 or 40 μM NH_4^+ under conditions in which the relative depletion of NH_4^+ is substantially more rapid than that of $CH_3NH_3^+$. Inhibition of $CH_3NH_3^+$ influx by NH_4^+ may be partially mediated by the membrane potential depolarization associated with NH_4^+ transport (Walker et al., 1979a, 1979b), which could also account for the complex nature of NH_4^+ inhibition of $CH_3NH_3^+$ influx.

Additional evidence for a common transport system is that net flux and short-term influx of both NH_4^+ and $CH_3NH_3^+$ were not significantly different (Fig. 4). These data indicate that, for plants grown under our conditions, efflux of either ion was negligible.

Table I. *Estimation of apparent K_m and V_{max} for NH_4^+ and $CH_3NH_3^+$ influx in the presence and absence of the other inhibiting ion using two different methods*

Linear regression analysis of Woolf-Augustinsson-Hofstee transformed data where $V = -K_m[S] + V_{max}$, and R and P are the correlation coefficient and probability for the linear regression, respectively. Hyperbolic regression analysis was conducted using the method of Wilkinson (1961). Values for apparent K_m and V_{max} are given ± calculated SE of regression. Values from experiments using $[^{15}N]NH_4^+$ and $[^{14}C]CH_3NH_3^+$ are for influx; all other values are for net flux.

Ion	Inhibitor	Linear Regression	R	P	K_m	V_{max}
					μM	μmol g^{-1} dry wt min^{-1}
NH_4^+	None	−7.04([S]) + 3.46	0.805	0.015	10.4 ± 2.2	3.64 ± 0.17
$^{15}NH_4^+$	None	−9.04([S]) + 3.30	0.875	0.006	10.9 ± 2.3	3.39 ± 0.14
$^{15}NH_4^+$	100 μM $CH_3NH_3^+$	−16.01([S]) + 2.98	0.783	0.019	23.5 ± 8.7	3.21 ± 0.29
$^{15}NH_4^+$	500 μM $CH_3NH_3^+$	−30.14([S]) + 2.59	0.896	0.015	39.7 ± 15.5	2.74 ± 0.27
$CH_3NH_3^+$	None	−44.38([S]) + 3.24	0.764	0.002	128.9 ± 28.1	4.7 ± 0.40
$CH_3NH_3^+$	10 μM NH_4^+	−40.24([S]) + 1.78	0.665	0.048	65.7 ± 19.4	2.07 ± 0.20
$CH_3NH_3^+$	40 μM NH_4^+	−70.4([S]) + 1.17	0.245	0.318	65.0 ± 28.7	0.97 ± 0.18
$[^{14}C]CH_3NH_3^+$	None	−151.87([S]) + 4.42	0.604	0.122	62.9 ± 31.1	3.68 ± 0.59
$[^{14}C]CH_3NH_3^+$	10 μM NH_4^+	−70.36([S]) + 1.66	0.761	0.054	219.2 ± 134.0	3.03 ± 0.81

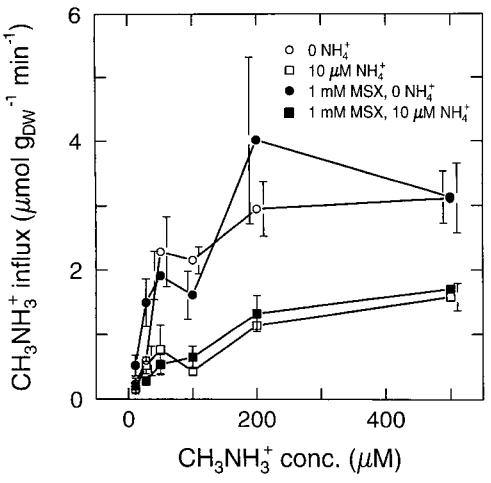

Figure 8. MSX effects on NH_4^+ inhibition of [^{14}C]$CH_3NH_3^+$ influx; $n = 3$ for all data. Shown is [^{14}C]$CH_3NH_3^+$ influx (μM $CH_3NH_3^+$ g^{-1} root dry weight [DW] min^{-1}) as a function of $CH_3NH_3^+$ concentration in the presence and absence of 1 mM MSX and 10 μM NH_4^+. Shown are the means ± SE with small error bars incorporated into the symbol.

This hypothetical common transport system seems to have a much greater affinity for NH_4^+ than for $CH_3NH_3^+$. The apparent K_m for NH_4^+ influx was about 10-fold less than that for $CH_3NH_3^+$ influx (Table I). Moreover, relatively low concentrations of NH_4^+ severely inhibit $CH_3NH_3^+$ influx (Fig. 6). Gln or some other product of NH_4^+ assimilation may act to control rates of NH_4^+ transport in maize; MSX treatments stimulated $^{15}NH_4^+$ influx in maize and barley roots (Jackson et al., 1993; Lee and Ayling, 1993). To test whether some product of NH_4^+ assimilation might also be responsible for NH_4^+ inhibition of $CH_3NH_3^+$ transport in tomato roots, we treated some plants with 1 mM MSX. Treatment with 1 mM MSX appeared to inhibit NH_4^+ assimilation (Fig. 7) in a manner consistent with previous studies (Fentem et al., 1983). The MSX treatment neither alleviated NH_4^+ inhibition of [^{14}C]$CH_3NH_3^+$ influx (Fig. 8) nor stimulated [^{14}C]$CH_3NH_3^+$ influx in the absence of NH_4^+. Thus, under our conditions, decreased root Gln and increased internal NH_4^+ did not appear to affect $CH_3NH_3^+$ transport. Measurement of MSX effects on NH_4^+ influx under our conditions would be necessary to determine whether there is any difference in the sensitivity of $CH_3NH_3^+$ and NH_4^+ influx to changes in levels of NH_4^+ metabolites.

In *Lemma gibba*, a linear component to NH_4^+ transport into fronds became apparent at concentrations greater than 100 μM NH_4^+ (Ullrich et al., 1984). Here, no linear component to NH_4^+ or $CH_3NH_3^+$ transport was evident over the concentration range used. The linear component to $^{13}NH_4^+$ transport in rice becomes significant only at concentrations of 1 mM NH_4^+ or higher (Wang et al., 1993). Measurements of NH_4^+ and $CH_3NH_3^+$ influx in this concentration range would be necessary to determine whether there is a similar linear component to transport of NH_4^+ and $CH_3NH_3^+$ in tomato, but such concentrations can be toxic with long exposure (Bloom, 1989).

Because NH_4^+ and $CH_3NH_3^+$ appear to share a common transport system in tomato, $CH_3NH_3^+$ should prove useful as an NH_4^+ analog in solution culture studies. Unfortunately, the interactions between NH_4^+ and $CH_3NH_3^+$ preclude using $CH_3NH_3^+$ in quantitative studies of plant NH_4^+ absorption from soil. Levels of NH_4^+ as low as 10 and 40 μM significantly inhibited $CH_3NH_3^+$ uptake (Table I; Fig. 8); therefore, accurate interpretation of labeling studies in the presence of soil NH_4^+ would depend on detailed knowledge of soil NH_4^+ distribution and concentration. Despite this limitation, [^{14}C]$CH_3NH_3^+$ or $CH_3NH_3^+$ might be used as an NH_4^+ tracer in soil when it is of paramount importance to distinguish between absorption of NO_3^- and NH_4^+. For example, determination of zones of active NH_4^+ absorption from the soil with [^{15}N]NH_4^+ as a tracer would be complicated by the conversion of [^{15}N]NH_4^+ to [^{15}N]NO_3^- by soil microorganisms; use of [^{14}C]$CH_3NH_3^+$ or $CH_3NH_3^+$ would avoid this problem. Our methods for nonsuppressed MPIC analysis of $CH_3NH_3^+$ and NH_4^+ may allow use of unlabeled $CH_3NH_3^+$ as a tracer of NH_4^+ in field studies in which radioactive labeling would not be appropriate.

ACKNOWLEDGMENTS

We thank Julie Bertholf, Richard Caldwell, Robert Carlson, John Finazzo, Louise Jackson, George Koch, Bernard Nicolaud, Daniel Schachtman, Carol Shennan, and David Smart for technical suggestions and assistance, and Ray Huffaker, Louise Jackson, Richard Jones, and David Smart for comments on the manuscript. David Smart designed the cuvettes for the 12-chamber system.

Received October 18, 1993; accepted January 24, 1994.
Copyright Clearance Center: 0032-0889/94/105/0435/08.

LITERATURE CITED

Arst HN Jr, Page MM (1973) Mutants of *Aspergillus nidulans* altered in the transport of methylammonium and ammonium. Mol Gen Genet **121:** 239–245

Bieleski RL, Turner NA (1966) Separation and estimation of amino acids in crude plant extracts by thin-layer electrophoresis and chromatography. Anal Biochem **17:** 278–293

Bloom AJ (1989) Continuous and steady-state nutrient absorption by intact plants. *In* LJ Winship, JG Torrey, eds, Application of Continuous and Steady-State Methods to Root Biology. Kluwer Academic, Dordrecht, The Netherlands, pp 147–163

Bloom AJ, Chapin FS III (1981) Differences in steady-state net ammonium and nitrate influx by cold and warm adapted barley varieties. Plant Physiol **68:** 1064–1067

Boussiba S, Dilling W, Gibson J (1984) Methylammonium transport in *Anacyctis nidulans* R-2. J Bacteriol **160:** 204–210

Carlson RM (1978) Automated separation and conductimetric determination of ammonia and dissolved carbon dioxide. Anal Chem **50:** 1528–1531

Cook RJ, Anthony C (1978) The ammonia and methylamine active transport system of *Aspergillus nidulans*. J Gen Microbiol **109:** 265–274

Epstein E (1972) Mineral Nutrition of Plants: Principles and Perspectives. Wiley, New York

Fentem PA, Lea PJ, Stewart GR (1983) Action of inhibitors of ammonia assimilation on amino acid metabolism in *Hordeum vulgare* L. (cv Golden Promise). Plant Physiol **71:** 502–506

Franco AR, Cardenas J, Fernandez E (1987) A mutant of *Chlamydomonas reinhardtii* altered in the transport of ammonium and methylammonium. Mol Gen Genet **206:** 414–418

Freund RJ, Littell RC, Spector PC (1986) SAS System for Linear Models, 1986 ed. SAS Institute, Cary, NC

Hackette SL, Skye GE, Burton C, Segel IH (1970) Characterization of an ammonium transport system in filamentous fungi with methylammonium-^{14}C as the substrate. J Biol Chem **245:** 4241–4250

Holtel A, Kleiner D (1985) Regulation of methylammonium transport in *Paracoccus denitrificans*. Arch Microbiol **142:** 285–288

Jackson RB, Caldwell MM (1992) Shading and the capture of localized soil nutrients: nutrient contents, carbohydrates, and root uptake kinetics of a perennial tussock grass. Oecologia **91:** 457–462

Jackson WA, Chaillou S, Morot-Gaudry JF, Volk RJ (1993) Endogenous ammonium generation in maize roots and its relationship to other ammonium fluxes. J Exp Bot **44:** 731–739

Kleiner D (1981) The transport of NH_3 and NH_4^+ across biological membranes. Biochim Biophys Acta **639:** 41–52

Lee RB, Ayling SM (1993) The effect of methionine sulphoximine on the absorption of ammonium by maize and barley roots over short periods. J Exp Bot **44:** 53–63

Macklon AES, Ron MM, Sim A (1990) Cortical cell fluxes of ammonium and nitrate in excised root segments of *Allium cepa* L.: studies using ^{15}N. J Exp Bot **41:** 359–370

McNaughton GS, Presland MR (1983) Whole plant studies using radioactive 13-nitrogen I. Techniques for measuring the uptake and transport of nitrate and ammonium ions in hydroponically grown *Zea mays*. J Exp Bot **34:** 893–902

Pateman JA, Dunn E, Kinghorn JR, Forbes EC (1974) The transport of ammonium and methylammonium in wildtype and mutant cells of *Aspergillus nidulans*. Mol Gen Genet **133:** 225–236

Pateman JA, Kinghorn JR, Dunn E, Forbes E (1973) Ammonium regulation in *Aspergillus nidulans*. J Bacteriol **114:** 943–950

Roon RJ, Even HL, Dunlop P, Larimore FL (1975) Methylamine and ammonia transport in *Saccharomyces cerevisiae*. J Bacteriol **122:** 502–509

Segel IH (1976) Biochemical Calculations. John Wiley & Sons, New York

Small H (1989) Ion Chromatography. Plenum Press, New York

Ullrich WR, Larsson M, Larsson C, Lesch S, Novacky A (1984) Ammonium uptake in *Lemna gibba* g1, related membrane potential changes, and inhibition of anion uptake. Physiol Plant **61:** 369–376

Walker NA, Beilby MJ, Smith FA (1979) Amine uniport at the plasmalemma of charophyte cells. I. Current-voltage curves, saturation kinetics, and effects of unstirred layers. J Membr Biol **49:** 21–55

Walker NA, Smith FA, Beilby MJ (1979) Amine uniport at the plasmalemma of charophyte cells. II. Ratio of matter to charge transported and permeability of free base. J Membr Biol **49:** 283–296

Wang MY, Siddiqi MY, Ruth TJ, Glass ADM (1993) Ammonium uptake by rice roots. II. Kinetics of $^{13}NH_4^+$ influx across the plasmalemma. Plant Physiol **103:** 1259–1267

Wilkinson BN (1961) Statistical estimations in enzyme kinetics. Biochem J **80:** 324–332